Electronic Supplementary Information

Exciton diffusion in monolayer and bulk $MoSe_2$

Nardeep Kumar,[a] Qiannan Cui,[a] Frank Ceballos,[a] Dawei He,[b] Yongsheng Wang,*[b] and Hui Zhao*[a]

[a] Department of Physics and Astronomy, The University of Kansas, Lawrence, Kansas 66045, USA.
E-mail: huizhao@ku.edu
[b] Key Laboratory of Luminescence and Optical Information, Ministry of Education, Institute of Optoelectronic Technology, Beijing Jiaotong University, Beijing 100044, China.
Email: yshwang@bjtu.edu.cn

1. Relation between differential reflection and exciton density

Figure S1 shows schematically the sample structure, which is composed of layers of $MoSe_2$, SiO_2, and Si, with thicknesses of d_i and complex indices of refraction of $\tilde{n}_i = n_i + \alpha_i j$, as labeled in the figure. The thickness of Si layer is treated as infinity since it is much longer than the absorption depth of the probe in Si. The reflection amplitude at each interface is obtained by Snell's Law, as shown on the right side of the figure. Adding all the reflected fields, we obtain the reflection coefficient,

$$R = \left| \frac{r_1 \exp[i(\phi_1+\phi_2)] + r_2 \exp[-i(\phi_1-\phi_2)] + r_3 \exp[-i(\phi_1+\phi_2)] + r_1 r_2 r_3 \exp[i(\phi_1-\phi_2)]}{\exp[i(\phi_1+\phi_2)] + r_1 r_2 \exp[-i(\phi_1-\phi_2)] + r_1 r_3 \exp[-i(\phi_1+\phi_2)] + r_2 r_3 \exp[i(\phi_1-\phi_2)]} \right|^2, \quad (1)$$

where the phase shift in each layer is $\phi_{1(2)} = 2\pi d_{1(2)} n_{1(2)} / \lambda$.

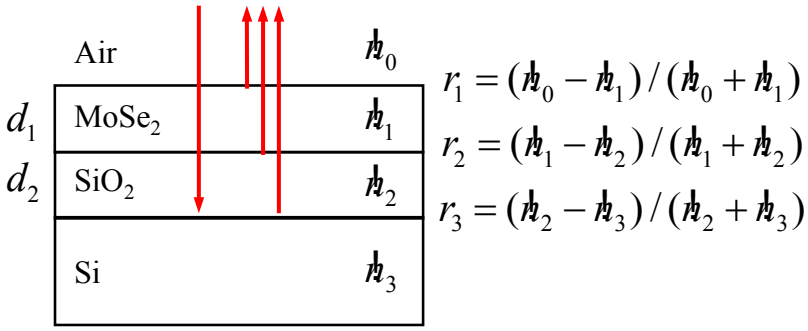

Figure S1: Schematics showing the multilayer reflection of the probe beam, and the corresponding parameters determining the reflection coefficient

We use Eq. (1) to calculate the linear reflection coefficient of the probe, R_0. The excitons injected by the pump pulse in $MoSe_2$ layer will change $\tilde{n}_1$, and therefore the R. Generally speaking, the excitons change both the real and the imaginary parts of $\tilde{n}_1$. However, since in the measurements the probe is tuned to the exciton absorption line, we expect the change in absorption, i.e. the imaginary part, contributes more.

We numerically exam the relation between the differential reflection and differential absorption by using Eq. (1). For a given value of differential absorption, we calculate the corresponding R, and then obtain the differential reflection. The result is plotted in Fig. S2. Clearly, for small magnitudes of differential absorption (< 0.1), the relation is approximately linear. In our actual measurements, the magnitude of the differential reflection signal is about 10^{-4}, which indicates a differential absorption of the same order. Hence, it is safe to conclude that the differential reflection measured is proportional to the differential absorption. We also confirmed, using the same procedure, that the differential reflection is proportional to the change in the index of refraction, so long as the differential reflection signal is small (< 0.1)

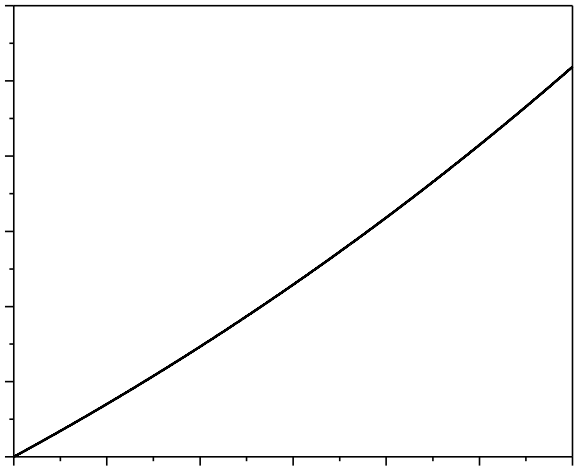

Figure S2: Differential reflection as a function of differential absorption calculated by using Eq. (1)

Under the condition that the injected exciton density is much smaller than the saturation density, the differential absorption is proportional to the exciton density. Since in our measurements the change in absorption coefficient is a small fraction of the linear absorption coefficient (10^{-4}), we know that the injected exciton density is much smaller than the saturation density. Therefore, we establish the linear relation between the differential reflection and the exciton density.

2. Drift-diffusion model and exciton density profiles

The spatiotemporal dynamics of the excitons injected by the tightly focused pump pulse is described by the classical diffusion equation,

$$\frac{\partial N(r,t)}{\partial t} = D\nabla^2 N(r,t) - \frac{N(r,t)}{\tau}.$$

With the initial condition of

$$N(r,t=0)=N_0 e^{-\frac{r^2}{\sigma_0^2}},$$

Its solution is

$$N(r,t)=\frac{\sigma_0^2 N_0}{\sigma_0^2+4Dt}e^{-\frac{t}{\tau}}e^{-\frac{r^2}{\sigma_0^2+4Dt}}.$$

Hence, the spatial profile of the exciton density remains the Gaussian shape, with a width that increases with time.

The above equation is used to fit the measured spatial profiles. Figure S3 shows a few examples. Clearly, the fits are satisfactory at all the probe delays. No deviation from the expected Gaussian shape is observed.

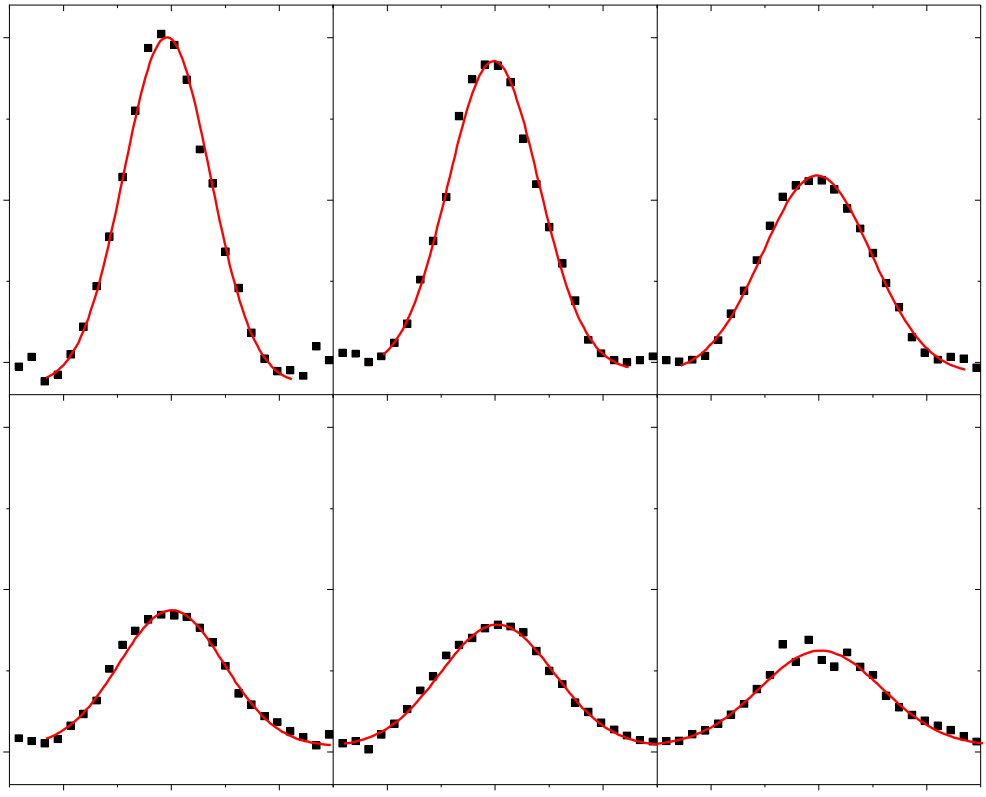

Figure S3: Exciton density profiles measured at several probe delays (as labeled in each panel) and the corresponding Gaussian fits (solid red lines)

Due to the finite size of the probe spot, the measured density profiles are convolutions of the actual density profiles and the probe intensity profile, which is also a Gaussian function,

$$I_p(r) = I_0 e^{-\frac{r^2}{\sigma_p^2}}.$$

The convolution of the two Gaussian functions remains Gaussian shape. The width of the measured profile at a certain probe delay is related to the actual profile width by $\sigma^2_{measured}(t) = \sigma^2_{actual}(t) + \sigma^2_p$. Hence, the effect of the finite probe spot is simply to add a constant to both sides of the broadening equation, σ^2_p. It does not change the slope, which is used to determine the diffusion coefficient.

When the centers of the pump and probe spots overlap (defined as $x = 0$), the decay of N is caused by both the exciton recombination and the diffusion of excitons out of the probe spot. By performing a convolution between the exciton density profile and the probe intensity profile, we find that the evolution of the measured N at x = 0 is

$$N(x=0) = \frac{A}{\sigma_p^2 + \sigma_0^2 + 4Dt} e^{-\frac{t}{\tau}},$$

where A is a constant. When analyzing the data, we first use the broadening of the profile to determined the D, and then fit the measured $N(x = 0)$ with the above equation to determine the exciton lifetime, with the known D.